Journal of Molecular Graphics and Modelling 27 (2008) 217–224

Contents lists available at ScienceDirect

Journal of Molecular Graphics and Modelling

journal homepage: www.elsevier.com/locate/JMGM

Molecular recognition of Docosahexaenoic acid by peroxisome proliferator-activated receptors and retinoid-X receptor α

Osman A.B.S.M. Gani, Ingebrigt Sylte *

Department of Pharmacology, Institute of Medical Biology, Faculty of Medicine, University of Tromsø, N-9037 Tromsø, Norway

ARTICLE INFO

Article history:
Received 25 February 2008
Received in revised form 21 April 2008
Accepted 22 April 2008
Available online 29 April 2008

Keywords:
Docosahexaenoic acid
Antidiabetic drug
Docking
MD simulations
PPARs

ABSTRACT

The family of peroxisome proliferator-activated receptors (PPARs) is the molecular target of synthetic antidiabetic and hypolipidemic drugs. The side effects of these drugs are limiting their use in patients with high lipid levels. Natural compounds, like Docosahexaenoic acid (DHA) from fish oil, have beneficial effects in the treatment of metabolic diseases, and several DHA derivatives are known to activate PPAR genes. Experimental studies on affinities of DHA and its derivatives for PPARs are not available. In the present study we are therefore using computational docking, molecular dynamics simulation, and several scoring programs to predict affinities and binding modes of DHA for PPARs and retinoid-X receptor α, which is the DNA binding partner of PPARs. The calculations indicated that DHA binds to PPARs and the retinoid-X receptor α with high affinity, and that different PPARs exhibited different structural effects on the first four carbons atoms of DHA. Our data indicate that the beneficial health effects of DHA may be obtained by high affinity binding to the PPARs.

1. Introduction

Peroxisome proliferator-activated receptors (PPARs) are known as physiological sensors of glucose and lipid homeostasis. The three isotypes of PPARs (PPARα, PPARδ, and PPARγ) belong to the superfamily of nuclear receptors. Fatty acids and eicosanoids are natural PPAR agonists [1,2]. Activated PPARs form complexes with a coactivator and retinoid-X receptor α (RXRα), and the resulting complex binds the DNA of the target genes [3]. RXRα is also a member of the nuclear receptor superfamily. Several synthetic drugs are also known as PPAR agonists (Chart 1). The fibrates are hypolipidemic drugs which act as PPARα agonists, while the glitazones are antidiabetic drugs which act as PPARγ agonists [4]. Type-2 diabetes and metabolic syndrome are often associated with high lipid and glucose levels in the blood, and therefore dual PPARα/γ agonists (such as muraglitazar) have also been developed.

Due to the side effects associated with synthetic PPAR agonists [5–7], naturally originated ligands and their derivatives have gained increasing focus. Docosahexaenoic acid (DHA), which is a fish oil component, has traditionally been used as functional food against metabolic disorders. Recently, DHA and some of its derivatives were also found to activate PPARα and PPARγ genes [8,9]. Although the balance between PPARα and PPARγ affinities is important in the design of effective dual agonists [4], binding affinities of DHA and its derivatives for PPARs are not available.

Experimental determination of binding affinities of fatty acids is problematic and gives uncertain results due to (a) poor solubility of fatty acids, (b) lack of radiolabel ligands, and (c) contaminants from recombinant proteins [10]. Scintillation proximity assays indicated that long chain fatty acids bind PPARα with an affinity in the range of 5–10 μM [2], while fluorescent binding assays reported a range of 5–17 nM [11]. Binding affinities in the nM range correspond to the physiological concentrations (7–50 nM) [12]. Contaminants from recombinant proteins are also believed to downgrade the affinities in the experimental studies [10].

In this study, we have used computational approaches to study the molecular interactions and affinities of DHA and the antidiabetic drugs rosiglitazone and pioglitazone for PPARs and RXRα.

2. Methods

2.1. Ligand–receptor docking

The ligand binding domains of PPARα (PDB ID 1I7G, chain-A), PPARγ (PDB ID 1FM6, chain-B), PPARδ (PDB ID 3GWX, chain-D), and RXRα (PDB ID 1MV9, chain-A) were loaded into the Internal Coordinate Mechanics (ICM) [13] v.3.0 program from the Protein Data Bank (PDB). Hydrogen atoms were added and optimized using

* Corresponding author. Tel.: +47 77644705; fax: +47 77645310.
E-mail address: Ingebrigt.sylte@fagmed.uit.no (I. Sylte).

1093-3263/$ – see front matter © 2008 Elsevier Inc. All rights reserved.
doi:10.1016/j.jmgm.2008.04.008

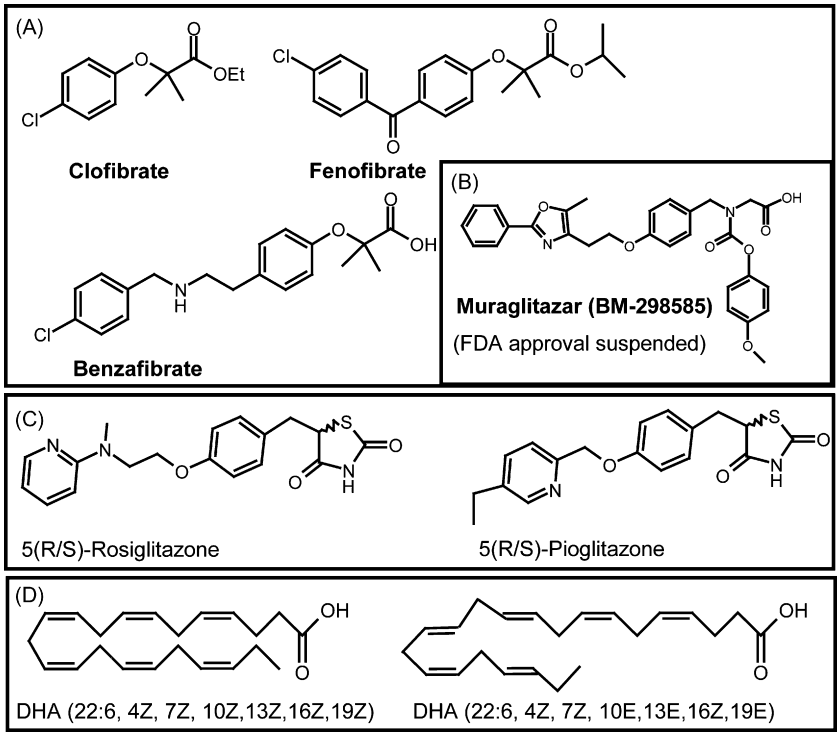

Chart 1. PPAR agonists. (A) PPARα agonists (marketed drugs), (B) dual PPARα/γ agonists (in clinical trail), (C) PPARγ agonists (marketed drugs), and (D) DHA.

the ECEPP/3 [14] force field of ICM. In all receptors, the active site histidine was protonated at both the N_δ and Nε atoms to enhance the possibility of hydrogen bonds with the ligands as seen in the X-ray crystallographic complexes [15–17]. A grid map that included the active site amino acids was calculated for the receptors. Coordinates of two DHA isomers (all-*cis* DHA and *cis*/*trans* DHA) and 5(*S*)-rosiglitazone were extracted from PDB IDs 1FDQ, 1MV9, and 1FM6, respectively. Initial models of 5(*R*)-rosiglitazone and 5(*R*/*S*)-pioglitazone were modeled with ICM. The ligands were assigned partial atomic charges according to the MMFF94 force field [18].

Flexible ligand docking was performed on rigid receptors with grid potentials. For each ligand, a stack of the 20 ligand–receptor complexes with low docking energies (ICM docking energy (ICM-DE)) was stored automatically. Each complex was manually examined, and was accepted based on the following criteria: (a) no van der Waals overlap between the ligand and amino acids of the receptor, and (b) oxygen atoms of the ligand should form hydrogen bonds with surrounding polar amino acids in the receptor as observed in the X-ray structures. According to these X-ray crystallographic complexes, following amino acids should form a H-bonding network with the ligand: PPARα—S280, Y314, H440 and Y464; PPARγ—S289, H323, H449 and Y473; PPARδ—H323, H449 and H449; and RXRα—R316 and A327 (main chain oxygen atoms). All-*cis* DHA was docked into PPARα, PPARγ, PPARδ and RXRα. *cis*/*trans* DHA was docked into PPARα and PPARγ, while glitazones were docked into PPARα, PPARγ and PPARδ.

2.2. Scoring

The accepted poses from docking of all-*cis* DHA and *cis*/*trans* DHA into PPARα and PPARγ were scored by five different scoring programs (in addition to ICM-DE): two force-field-based—ICM binding energy (ICM-BE) [19] and DOCK (v.5.3) [20]; two empirical—X-SCORE (v.1.2.1) [21] and SCORE (v.2.0) [22]; and one knowledge-based—DrugScore [23]. The default settings were used for each program. While ICM-BE (a macro termed *calcBindingEnergy*) attempts to calculate free energy of binding, others attempt to rank the poses according to their interaction energies with the receptor. The poses after docking of all-*cis* DHA into RXRα and PPARδ, and the poses after docking of glitazones into PPARγ were scored by ICM-DE.

2.3. MD simulations and rescoring

Molecular dynamics (MD) simulations for 4 ns were performed with AMBER 8 [24] suit of programs on the following eight complexes:

- PPARα in complexes with all-*cis* DHA and *cis*/*trans* DHA;
- PPARγ in complexes with all-*cis* DHA, (5*R*) and (5*S*)-rosiglitazone and (5*S*)-pioglitazone;
- PPARδ in complex with all-*cis* DHA;
- RXRα in complex with all-*cis* DHA.

MD simulations were performed with both charged and neutral DHA. The starting complex for the simulation of PPARα with all-*cis* DHA was the one in Table 1 with lowest sum of rankings after scoring with different scoring functions. For other ligands no clear consensus was seen among scores of different scoring functions, so the pose with lowest ICM-BE was used as starting complex for MD simulations.

Duan et al. [25] force field was used for receptors, and the generalized force field (GAFF) was used for ligands. Electrostatic potentials were quantum mechanically calculated by the Gaussian98 [26] program using a HF/6-31G* basis set, and restrained electrostatic potential (RESP) [27] point charges were calculated by the ANTECHAMBER program of AMBER. To solvate, a rectangular box of TIP3P [28] water model was used. The box consisted of ~12,000 water molecules for receptor-ligand complexes and ~900 for a ligand molecule. Na^+ ions were used to neutralize the solvated systems. The molecular systems were energy minimized for 2500

Table 1
Scores of the accepted ICM poses of all-*cis* DHA to PPARα

Pose	ICM-DE	DOCK	DrugScore	SCORE	X-SCORE	ICM-BE	Rank
1	−57.71 (1)	−40.99 (6)	−540784 (2)	8.19 (3)	6.85 (1)	−13.53 (5)	18
2	−55.84 (2)	−17.53 (12)	−541000 (1)	9.32 (1)	6.8 (2)	−12.63 (8)	26
3	−55.62 (3)	−33.92 (10)	−539434 (3)	6.69 (12)	6.22 (11)	−15.68 (2)	41
4	−48.93 (4)	−42.14 (4)	−520280 (6)	7.89 (4)	6.65 (5)	−12.21 (10)	33
5	−47.63 (5)	−15.23 (11)	−519263 (7)	7.02 (9)	6.29 (10)	−13.45 (6)	48
6	−47.06 (6)	−38.72 (7)	−508161 (10)	6.73 (11)	6.08 (12)	−16.14 (1)	47
7	−46.79 (7)	−53.00 (2)	−521626 (5)	7.1 (7)	6.47 (9)	−13.78 (4)	34
8	−45.22 (8)	−41.54 (5)	−485345 (11)	8.38 (2)	6.63 (6)	−12.25 (9)	41
9	−41.59 (9)	−59.62 (1)	−512943 (9)	7.13 (6)	6.54 (7)	−14.71 (3)	35
10	−41.31 (10)	−43.49 (3)	−516504 (8)	6.76 (10)	6.53 (8)	−12.94 (7)	46
11	−36.71 (11)	−36.79 (9)	−531961 (4)	7.05 (8)	6.77 (3)	−10.38 (12)	47
12	−35.73 (12)	−37.70 (8)	−366802 (12)	7.49 (5)	6.73 (4)	−11.83 (11)	52
S.D.	±7.18	±19.78	±47415.73	±0.81	±0.24	±1.64	

ICM-BE and DOCK values are energies in kcal/mol. X-SCORE and SCORE correspond to pK_d. DrugScore ranks the poses relative to each other based on empirical knowledge. The values in the parentheses indicate rank of that individual pose by corresponding scoring function. Rank is sum of the rankings (values in the parentheses) by the different scoring function of an individual pose. S.D. denotes 'standard deviations'.

cycles, initially by *steepest decent* followed by *conjugate gradient* minimization methods. MD simulations were performed on a cluster of four processors (HP r× 4640/5670; 41.3/41.5 GHz Itanium2) with a parallelized SANDER program; 200 ps constant volume equilibration dynamics followed by 3.8 ns constant pressure (NPT) dynamics at 300 K. SHAKE [29] was used to restraint bonds containing a hydrogen atom. Periodic boundary condition, and Berendsen temperature coupling [30] were also applied. The temperature was controlled by using a collision frequency of 1.0 ps^{-1}, while the pressure was 1 atm with a relaxation time of 2 ps. The particle mesh Ewald method was used for calculating long range electrostatic interactions [24]. The time step during the simulations was 2 fs. Non-bonding cut-off radius of 9 Å was chosen with non-bonded pair lists updated every 15 steps. Coordinate sets were sampled each 5 ps. ICM and VMD [31] were used to visualize the simulations. Fluctuations of potential energies, total energies and temperature were monitored to ensure stability during simulations.

After MD simulations, the average structures from every 100 ps during the last ns simulation (3–4 ns) of the complexes of all-*cis* DHA with PPARα and PPARγ were rescored by the different scoring functions. The coordinate sets sampled during the last ns (3–4 ns) were used to calculate binding energies by the linear interaction energy LIE method [32]. The coefficients used by the LIE equations were adopted from Hansson et al. [33]; $\alpha = 0.181$ for all ligands, but $\beta = 0.50$ for DHA and 0.43 for glitazones.

3. Results

3.1. Docking and scoring

We used six scoring programs to score the ICM generated docking poses of all-*cis* DHA (22:6 4Z, 7Z, 10Z, 13Z, 16Z, 19Z) and *cis*/*trans* DHA (22:6 4Z, 7Z, 10E, 13E, 16Z, 19E) in PPARα and PPARγ. Consensus, in terms of ranking the poses, among different scoring functions was only seen for docking of all-*cis* DHA into PPARα (Table 1). For this docking, the top-ranked pose by ICM-DE was also validated as the best by the scoring programs by consensus (Table 1), and that docking pose was used as the starting complex for MD simulation. A similar consensus was not observed for all-*cis* DHA after docking into PPARγ (Table 2) and for the complexes of *cis*/*trans* DHA (data not shown), and the best scored poses by ICM-BE were used as the starting complex for MD simulations. The top-ranked binding poses of all-*cis* DHA in PPARα (as a representative for PPARs) and RXRα is shown in Fig. 1.

From MD simulations of all-*cis* DHA with PPARα and PPARγ, the average coordinates from every 100 ps during the last ns simulation (3–4 ns) were rescored by different scoring functions. These average complexes were scored consistently by ICM-BE, SCORE, and X-SCORE. DOCK showed moderate inconsistency, while DrugScore showed highly inconsistent results (Table 3). A similar trend was also seen for the scoring of the average complexes between 3 and 4 ns MD of PPARγ with all-*cis* DHA (data not shown).

Previous experimental studies showed that PPARγ binds rosi- and pioglitazone with inhibition constant (K_i) values of 47 nM and 1.3 μM, respectively [34]. Roughly, these K_i values correspond to binding energies of about −10 and −8 kcal/mol, respectively. Our calculations indicated that both ICM-BE and LIE calculations overestimated the affinities of rosi- and pioglitazone (Table 4). A hydrogen bond network, as observed in X-ray crystallographic complex [15], was used as criterion for accepting the docked poses. A cut-off of 3.5 Å was used to define hydrogen bonds. Rosi- and pioglitazone were docked into the PPARs, but did not form acceptable docking poses with PPARα and PPARδ. Complexes of

Table 2
Scores of the accepted ICM poses of all-*cis* DHA to PPARγ

Pose	ICM-DE	DOCK	DrugScore	SCORE	X-SCORE	ICM-BE	Rank
1	−44.48 (1)	−37.95 (2)	−545022 (5)	6.39 (6)	6.69 (5)	−11.34 (1)	20
2	−43.73 (2)	−36.85 (3)	−575390 (4)	6.29 (7)	6.75 (4)	−10.13 (6)	26
3	−41.09 (3)	−44.29 (1)	−529786 (7)	8.05 (1)	6.47 (7)	−10.31 (3)	22
4	−27.90 (4)	−32.08 (4)	−582926 (1)	7.48 (2)	6.96 (1)	−10.01 (7)	19
5	−27.54 (5)	−2.13 (5)	−488034 (2)	7.22 (3)	6.91 (2)	−11.26 (2)	19
6	−27.37 (6)	19.26 (6)	−545981 (3)	6.66 (5)	6.91 (3)	−10.22 (5)	28
7	−26.39 (7)	101.42 (7)	−507633 (6)	6.69 (4)	6.55 (6)	−10.31 (4)	34
S.D.	±8.52	±52.12	±34167.71	±0.64	±0.19	±0.55	

The values obtained by the different scoring functions are explained in Table 1.

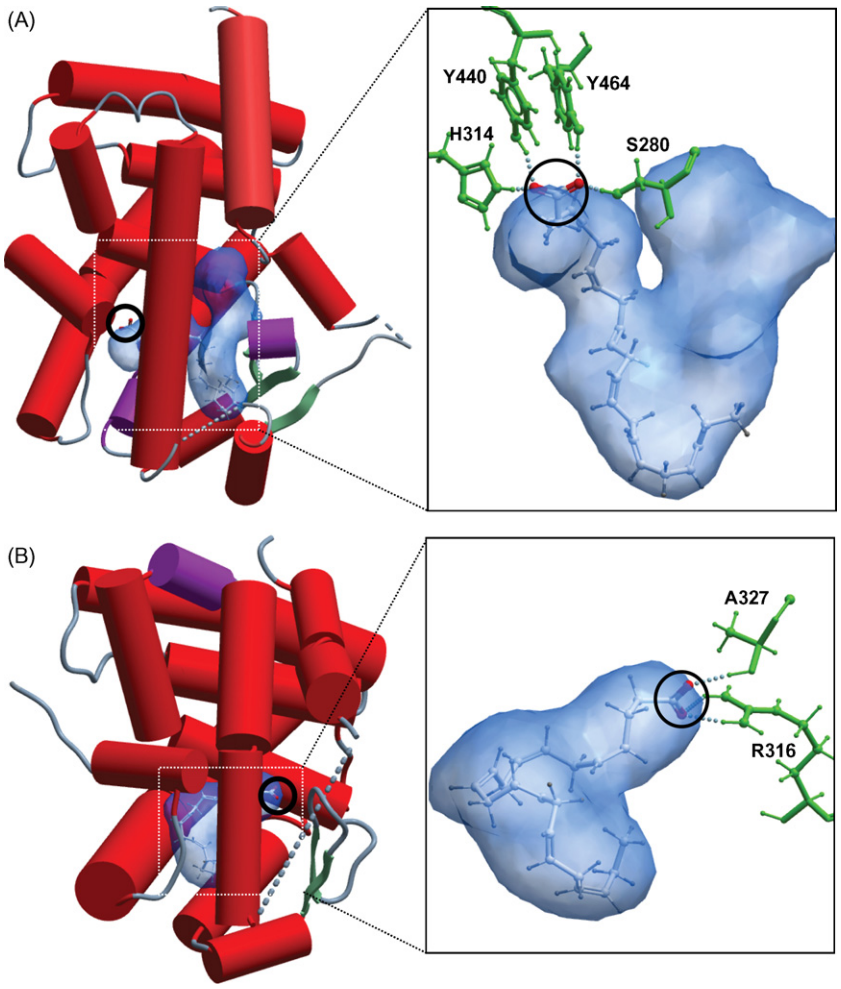

Fig. 1. Binding mode of all-*cis* DHA with PPARα and RXRα. The binding mode in PPARα is shown as a representative for the PPARs. (A) The top-ranked binding pose of DHA in PPARα (PDB ID 1I7G, chain A). Color coding of secondary structures: α-helices in red, β-strands in green, and loops in cyan. Blue surface object in the box shows ligand binding pocket and stick model of DHA. An enlarged view of the ligand binding pocket is shown to the right, where the amino acids important for hydrogen bonds (dotted lines) with DHA are labelled. The circle shows the carboxylic group of DHA that forms hydrogen bonds with the receptor. (B) Top-ranked pose of DHA in the binding site of RXRα (PDB ID 1MV9, chain A). Descriptions of the secondary structures and binding site are as in A.

rosi- and pioglitazone with PPARα and PPARδ were therefore not considered for further calculations.

Negatively charged DHA showed much stronger interaction energies than neutral DHA. Table 4 also shows that binding energies with ICM-BE were much closer to the LIE values with neutral DHA than with negatively charged DHA. For PPARγ, we found a LIE of −12.88 kcal/mol for neutral all-*cis* DHA, and −33.56 kcal/mol for charged all-*cis* DHA. Hence, LIE values with negatively charged DHA seemed unlikely.

Table 3
Scores of MD simulated average poses of all-*cis* DHA with PPARα

Interval (ns)	DOCK	DrugScore	SCORE	X-SCORE	ICM-BE
3.0–3.1	−47.56	−634630	9.45	6.90	−10.39
3.1–3.2	−46.15	−597355	8.84	6.70	−10.66
3.2–3.3	−39.77	−595564	8.40	6.89	−9.68
3.3–3.4	−43.79	−585769	9.45	6.79	−9.78
3.4–3-5	−47.89	−587426	9.17	6.74	−10.66
3.5–3.6	−43.53	−596227	8.24	6.55	−10.17
3.6–3.7	−30.11	−601607	9.07	6.84	−9.30
3.7–3.8	−43.60	−627726	9.01	6.92	−9.55
3.8–3.9	−43.02	−623442	8.84	6.89	−9.31
3.9–4.0	−33.75	−622581	8.57	6.88	−9.82
S.D.	±0.51	±17976.52	±0.41	±0.12	±0.51

Energy minimized average structures between 3 and 4 ns of MD simulations were scored. The values obtained by the different scoring functions are explained in Table 1.

3.2. The interactions of DHA isomers with PPARα

The binding energies with both ICM-BE and LIE indicated that PPARα has higher affinity for *cis*/*trans* DHA than for all-*cis* DHA (Table 4). Although both DHA isomers formed similar hydrogen bonds with PPARα, *cis*/*trans* DHA exhibited stronger van der Waals interactions than all-*cis* DHA. The former formed 22 contacts within 3.7 Å of the receptor, while the latter formed 16 receptor contacts within similar distances. The amino acids C275, T279, Q282, L321, and Y334 formed extra contacts with *cis*/*trans* DHA compared with all-*cis* DHA. Average van der Waals interactions during MD (3–4 ns) were about −50 kcal/mol for both DHA isomers, while the electrostatic interactions were about −26 and −18 kcal/mol for *cis*/*trans* DHA and all-*cis* DHA, respectively.

3.3. DHA versus glitazones

LIE showed that both enantiomers of rosiglitazone have stronger affinities than 5(*S*)-pioglitazone for PPARγ (Table 4). However, ICM-BE suggested that 5(*R*)-rosiglitazone showed

Table 4
Binding energies of MD simulated poses

Receptor–ligand	ICM-BE	LIE (neutral ligand)	LIE (charged ligand)	IC_{50}/K_i (μM)
PPARα–DHA (*cis*/*trans*)	−13.43	−18.75	−32.50	
PPARα–DHA (all-*cis*)	−12.30	−16.09	−27.32	
PPARγ–DHA (all-*cis*)	−11.13	−12.88	−33.56	
PPARγ–rosiglitazone (5*R*)	−13.13	−19.90		2.000[a]
PPARγ–rosiglitazone (5*S*)	−11.01	−13.14		0.030[a]
PPARγ–pioglitazone (5*S*)	−11.35	−12.24		
PPARγ–rosiglitazone (racemate)				0.047[b]
PPARγ–pioglitazone (racemate)				1.300[b]
PPARδ–DHA (all-*cis*)	−12.72	−16.80	−22.95	
RXRα–DHA (all-*cis*)	−12.65	−10.00	−29.19	

The binding energies ICM-BE were calculated for the final coordinate set after 4 ns MD simulations. Coordinate sets for LIE analysis were taken from last ns (3–4 ns) MD simulations.
[a] Experimental IC_{50} [40] values of individual enantiomers.
[b] Experimental K_i [35] values of racemates.

stronger affinity than 5(*S*)-pioglitazone for PPARγ, while 5(*S*)-rosiglitazone and 5(*S*)-pioglitazone exhibited similar affinities. Both ICM-BE and LIE showed that 5(*R*)-rosiglitazone exhibited stronger affinity than 5(*S*)-rosiglitazone for PPARγ.

Both ICM-BE and LIE showed that the binding affinity of all-*cis* DHA for PPARγ was in the same range as those with 5(*S*)-rosiglitazone and 5(*S*)-pioglitazone, but weaker than for 5(*R*)-rosiglitazone. Also, both ICM-BE and LIE suggested that all-*cis* DHA binds strongly to PPARδ. All-*cis* DHA also exhibited considerable affinity for RXRα, although LIE was weaker than those for PPARs (Table 4).

3.4. Determinants of DHA binding to PPARs

The variation of torsion angles of all-*cis* DHA in complex with different PPARs was monitored during 4 ns MD simulations (Fig. 2). These torsions varied in the first four carbon atoms of all-*cis* DHA. The torsion angles in the repeating unit of DHA (methyl groups flanked by double bonds) remained near to eclipsed conformations during MD simulations, but the two torsion angles at the end of DHA deviated largely from eclipsed conformation.

In general the monitored torsional angles were most flexible during MD with PPARα, and the angles O–C1–C2–C3 and C4–C5–C6–C7 were fluctuating during the entire MD. During the MD with PPARγ the monitored torsional angles were quite stable after 1 ns of MD. For PPARδ the torsional angles, except for C1–C2–C3–C4, were also quite stable after 1 ns of MD.

4. Discussion

4.1. Binding efficiency of DHA

Although DHA remains in nature as all-*cis* isomer, we also studied the interactions of the *cis*/*trans* isomer with PPARα. The reason for that was that *cis*/*trans* DHA is present in complex with RXRα in the PDB (1MV9), and that its receptor interactions may be of importance for the design of DHA derivatives.

Six scoring functions were used to evaluate the docking poses. By using several scoring programs we might compensate for potential errors by each program, and such a strategy has been reported to improve the predictions [35,36]. Consensus among the scoring functions in identifying a specific pose was therefore considered as an indication of the most reliable (native-like) docking pose. For docking of two DHA isomers into PPARγ we did not get any consensus among the scoring functions, which may suggest that several conformations of the isomers are possible in the PPARγ. However, docking of all-*cis* DHA into PPARα clearly identified a docking pose as the most reliable, which supports the use of several scoring functions for identifying the most reliable docking pose.

Scoring of MD simulated poses (Table 3) is believed to partly reflect the flexibility of the receptor during the binding process. To reduce computer time during MD, SHAKE was performed to restraint bonds containing hydrogen atoms. We are aware of that using SHAKE for NPT (constant pressure) calculations may induce errors such that estimated physical parameters will be slightly incorrect. However, SHAKE was used for bonds with a hydrogen atom, only. Berendsen temperature coupling was used during MD. The Berendsen method is robust, and therefore very feasible in the initial steps of NPT MD runs. A drawback with the method is that canonical ensembles cannot be constructed during sampling. This will only have minor impact on the final results in the present study. Therefore, we believe that applying SHAKE on bonds containing hydrogen atoms and Berendsen temperature coupling during NPT MD runs will not affect the relative interaction energies, since the LIE method is an approximation.

The scores after MD simulations showed consistencies (low standard deviations) with ICM-BE, SCORE and X-SCORE, which indicate that native-like reliable PPAR–DHA conformations are predicted by these functions.

To our knowledge, the experimental affinities of DHA for PPARs and RXRα are not reported. LIE predicted strong DHA affinities for PPARs and RXRα. The LIE results obtained with neutral DHA seemed more promising than with charged DHA. Even with the neutral DHA, the LIE values indicate that the affinities are in the nM range, which are supported by the fluorescent binding assays [11]. The overestimations with charged ligand are also supported by the previously published data, which observed overestimation of the LIE values with charged biotin analogues [37]. The free energy of binding corresponds to the difference between the desolvation energy and ligand–protein complex energy. Charged ligands correspond to very large desolvation energies with the possibility of large numerical errors, and the calculation of the differences may therefore also inherit large numerical errors. An overestimation may also be expected due to charged groups at the receptor binding site [38].

LIE and ICM-BE values indicated that *cis*/*trans* DHA binds with stronger affinity than all-*cis* DHA to PPARα (Table 3). The calculations indicated that difference in the electrostatic interactions was the main contributor to the higher affinity of *cis*/*trans* than of all-*cis* DHA. The predicted binding energies of glitazones for PPARγ (Table 4), specifically LIE values, are in agreement with experimental data which show that rosiglitazone has stronger affinity for PPARγ than pioglitazone [34]. The calculations predicted that 5(*R*)-rosiglitazone has stronger binding affinity than 5(*S*)-rosiglitazone for PPARγ, which is contradictory to

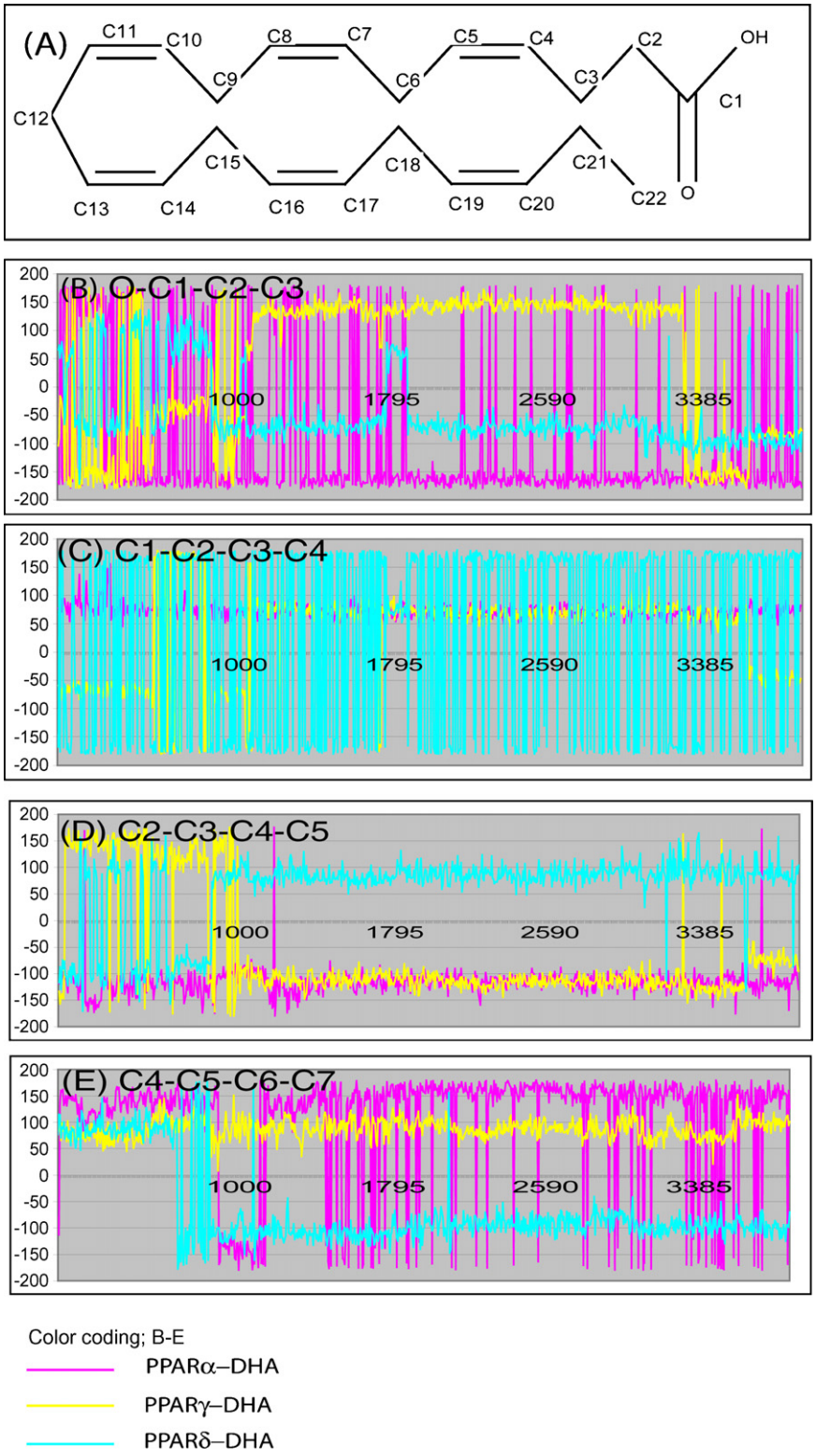

Fig. 2. Torsion angles of DHA in complex with the PPARs. (A) The structure of all-*cis* DHA. (B–D) Distribution of torsion angles within first four carbon atoms of DHA during 4 ns MD simulations in complex with the PPARs. (E) Representative example of distribution of torsion angles within the repeating unit (a methyl group flanked by double bonds) of DHA during simulations. In panels B–E, the *X*-axis shows time in picoseconds, while the *Y*-axis shows torsion angle in degrees.

experimental IC_{50} values [39]. Although in animal model both enantiomers showed equivalent activity [40]. Recently, it has been a focus on PPARδ agonists as potential drugs against metabolic syndrome [41]. Table 4 indicates that all-*cis* DHA also has high affinity for PPARδ, which may contribute to the beneficial effects of DHA on health risk factors associated with metabolic syndrome. All-*cis* DHA also had high affinity for RXRα, which indicates that DHA binding to either of the partners in PPAR–RXR complex can activate the heterodimers. Binding to both partners of the complex may also give synergistic effects [42,43].

Rosi- and pioglitazone did not form acceptable binding poses with PPARα and PPARδ, which is in agreement with experimental studies showing that glitazones do not bind PPARα and PPARδ [44]. The X-ray structures show that the side chain of Y314 in PPARα forms steric clash with the head group of glitazones, and narrow binding region of PPARδ cannot accommodate this head group of glitazones. Thus, binding of the giltazones with PPARα and PPARδ ultimately inhibited. Y314 is substituted as H323 in PPARγ, which forms hydrogen bonds with the glitazone head group.

4.2. Variations of binding of DHA to PPARs

The calculations showed that the torsion angles within first four carbon atoms of all-*cis* DHA varied among different PPAR–DHA complexes. Usually, PPAR ligands have three essential parts for optimal binding: (a) polar head group, (b) linker region, and (c) hydrophobic tail. In all complexes with the PPARs, the carboxylic head group of DHA was held by hydrogen bonds to the polar residues at the active site. Hence, changes in O–C1–C2–C3 torsion reflect rotation around C2–C3 bond axis. This torsion remained almost stable in PPARδ (Fig. 2), which indicates a narrow polar region of PPARδ active site [45]. However, with PPARα and PPARγ this torsion angle was varying during the MD simulations, and therefore substitution on either or both α and β carbons of DHA may form favorable additional interactions with the receptor, and increase the affinity.

The torsion angle C1–C2–C3–C4 also varied among different PPARs. In PPARα and PPARγ, it remained stable around 70–80°; while in PPARδ this angle varied due to rotation of the C3–C4 bond (Fig. 2). The structural flexibility of all-*cis* DHA in PPARδ supports that both 'tail-up' and 'tail-down' conformation of DHA are possible in the hydrophobic regions of the receptor [46]. Such movements of DHA are restricted in PPARα and PPARγ. The flat liker region of the known PPARα/PPARγ ligands also supports rigidity of C1–C2–C3–C4 torsion [15]. As expected, the torsion angle C2–C3–C4–C5 of DHA was stable during MD of all PPAR subtypes (Fig. 2), and thereby the bond angle C2–C3–C4 also remained stable at ∼111°. Eclipsed conformations in the repeating units are supported by a previous QM calculation [46]. Large structural fluctuations of torsion angle C19–C20–C21–C22 at the end of the chain were seen during MD simulations with all PPARs (data not shown), and indicated that the tail did not have strong hydrophobic contact with the receptor residues.

5. Conclusions

The results obtained in this study suggest that DHA can bind with sufficient affinities to PPARs and RXRα, and therefore may transcript a broad spectrum of genes which reduces insulin resistance, high blood pressure, obesity, and the related risk factors of metabolic syndrome. We believe that this may be a reason for the beneficial effects of DHA in metabolic diseases, and therefore DHA is traditionally used as functional food. Substituents in α/β position of DHA may strengthen the contacts with the PPARα and PPARγ and enhance affinity. Hence, DHA derivatives may act as dual PPARα/γ agonists against diabetes and metabolic syndrome.

Acknowledgements

We greatly acknowledge Pronova Biocare AS, Norway, for economical support, and the Notur project for access to supercomputer facilities.

References

[1] S.A. Kliewer, S.S. Sundseth, S.A. Jones, P.J. Brown, G.B. Wisely, C.S. Koble, P. Devchand, W. Wahli, T.M. Willson, J.M. Lenhard, J.M. Lehmann, Fatty acids and eicosanoids regulate gene expression through direct interactions with peroxisome proliferator-activated receptors alpha and gamma, Proc. Natl. Acad. Sci. U.S.A. 94 (1997) 4318–4323.
[2] G. Krey, O. Braissant, F. L'Horset, E. Kalkhoven, M. Perroud, M.G. Parker, W. Wahli, Fatty acids, eicosanoids, and hypolipidemic agents identified as ligands of peroxisome proliferator-activated receptors by coactivator-dependent receptor ligand assay, Mol. Endocrinol. 11 (1997) 779–791.
[3] H. Keller, C. Dreyer, J. Medin, A. Mahfoudi, K. Ozato, W. Wahli, Fatty acids and retinoids control lipid metabolism through activation of peroxisome proliferator-activated receptor-retinoid X receptor heterodimers, Proc. Natl. Acad. Sci. U.S.A. 90 (1993) 2160–2164.
[4] T.M. Willson, P.J. Brown, D.D. Sternbach, B.R. Henke, The PPARs: from orphan receptors to drug discovery, J. Med. Chem. 43 (2000) 527–550.
[5] R.W. Nesto, D. Bell, R.O. Bonow, V. Fonseca, S.M. Grundy, E.S. Horton, M. Le Winter, D. Porte, C.F. Semenkovich, S. Smith, L.H. Young, R. Kahn, Thiazolidinedione use, fluid retention, and congestive heart failure: a consensus statement from the American Heart Association and American Diabetes Association, Circulation 108 (October) (2003) 2941–2948.
[6] S.E. Nissen, K. Wolski, Effect of rosiglitazone on the risk of myocardial infarction and death from cardiovascular causes, N. Engl. J. Med. 356 (2007) 2457–2471.
[7] C. Fievet, J.C. Fruchart, B. Staels, PPARalpha and PPARgamma dual agonists for the treatment of type 2 diabetes and the metabolic syndrome, Curr. Opin. Pharmacol. 6 (2006) 606–614.
[8] T. Itoh, I. Murota, K. Yoshikai, S. Yamada, K. Yamamoto, Synthesis of docosahexaenoic acid derivatives designed as novel PPARgamma agonists and antidiabetic agents, Bioorg. Med. Chem. 14 (2006) 98–108.
[9] L.N. Larsen, L. Granlund, A.K. Holmeide, L. Skattebol, H.I. Nebb, J. Bremer, Sulfur-substituted and alpha-methylated fatty acids as peroxisome proliferator-activated receptor activators, Lipids 40 (2005) 49–57.
[10] S.A. Fyffe, M.S. Alphey, L. Buetow, T.K. Smith, M.A. Ferguson, M.D. Sorensen, F. Bjorkling, W.N. Hunter, Recombinant human PPAR-beta/delta ligand-binding domain is locked in an activated conformation by endogenous fatty acids, J. Mol. Biol. 356 (2006) 1005–1013.
[11] Q. Lin, S.E. Ruuska, N.S. Shaw, D. Dong, N. Noy, Ligand selectivity of the peroxisome proliferator-activated receptor alpha, Biochemistry 38 (1999) 185–190.
[12] J.A. Hamilton, Fatty acid transport: difficult or easy? J. Lipid Res. 39 (1998) 467–481.
[13] R. Abagyan, M. Totrov, D. Kuznetsov, Icm – a new method for protein modeling and design – applications to docking and structure prediction from the distorted native conformation, J. Comput. Chem. 15 (1994) 488–506.
[14] G. Nemethy, K.D. Gibson, K.A. Palmer, C.N. Yoon, G. Paterlini, A. Zagari, S. Rumsey, H.A. Scheraga, Energy parameters in polypeptides. 10: Improved geometrical parameters and nonbonded interactions for use in the Ecepp/3 algorithm, with application to proline-containing peptides, J. Phys. Chem. 96 (1992) 6472–6484.
[15] P. Cronet, J.F. Petersen, R. Folmer, N. Blomberg, K. Sjoblom, U. Karlsson, E.L. Lindstedt, K. Bamberg, Structure of the PPARalpha and -gamma ligand binding domain in complex with AZ 242; ligand selectivity and agonist activation in the PPAR family, Structure (Camb.) 9 (2001) 699–706.
[16] P.F. Egea, A. Mitschler, D. Moras, Molecular recognition of agonist ligands by RXRs, Mol. Endocrinol. 16 (2002) 987–997.
[17] R.T. Gampe Jr., V.G. Montana, M.H. Lambert, A.B. Miller, R.K. Bledsoe, M.V. Milburn, S.A. Kliewer, T.M. Willson, H.E. Xu, Asymmetry in the PPARgamma/RXRalpha crystal structure reveals the molecular basis of heterodimerization among nuclear receptors, Mol. Cell 5 (2000) 545–555.
[18] T.A. Halgren, Merck molecular force field. 1: Basis, form, scope, parameterization, and performance of MMFF94, J. Comput. Chem. 17 (1996) 490–519.
[19] M. Schapira, M. Totrov, R. Abagyan, Prediction of the binding energy for small molecules, peptides and proteins, J. Mol. Recognit. 12 (1999) 177–190.
[20] S. Makino, I.D. Kuntz, Automated flexible ligand docking method and its application for database search, J. Comput. Chem. 18 (1997) 1812–1825.
[21] R. Wang, L. Lai, S. Wang, Further development and validation of empirical scoring functions for structure-based binding affinity prediction, J. Comput. Aided Mol. Des. 16 (2002) 11–26.
[22] Renxiao Wang, Liang Liu, Luhua Lai, Youqi Tang, A new empirical method for estimating the binding affinity of a protein–ligand complex, J. Mol. Model. 4 (1998) 379–394.
[23] H. Gohlke, M. Hendlich, G. Klebe, Knowledge-based scoring function to predict protein–ligand interactions, J. Mol. Biol. 295 (2000) 337–356.
[24] D.A. Case, T.A. Darden, T.E. Cheatham III, C.L. Simmerling, J. Wang, R.E. Duke, R. Luo, K.M. Merz, B. Wang, D.A. Pearlman, M. Crowley, S. Brozell, V. Tsui, H. Gohlke, J. Mongan, V. Hornak, G. Cui, P. Beroza, C. Schafmeister, J.W. Caldwell, W.S. Ross, P.A. Kollman, AMBER 8, University of California, San Francisco, CA, 2004.
[25] Y. Duan, C. Wu, S. Chowdhury, M.C. Lee, G. Xiong, W. Zhang, R. Yang, P. Cieplak, R. Luo, T. Lee, J. Caldwell, J. Wang, P. Kollman, A point-charge force field for molecular mechanics simulations of proteins based on condensed-phase quantum mechanical calculations, J. Comput. Chem. 24 (2003) 1999–2012.
[26] M.J. Frisch, G.W. Trucks, H.B. Schlegel, G.E. Scuseria, M.A. Robb, J.R. Cheeseman, J.A. Montgomery Jr., T. Vreven, K.N. Kudin, J.C. Burant, J.M. Millam, S.S. Iyengar, J. Tomasi, V. Barone, B. Mennucci, M. Cossi, G. Scalmani, N. Rega, G.A. Petersson, H. Nakatsuji, M. Hada, M. Ehara, K. Toyota, R. Fukuda, J. Hasegawa, M. Ishida, T.

Nakajima, Y. Honda, O. Kitao, H. Nakai, M. Klene, X. Li, J.E. Knox, H.P. Hratchian, J.B. Cross, V. Bakken, C. Adamo, J. Jaramillo, R. Gomperts, R.E. Stratmann, O. Yazyev, A.J. Austin, R. Cammi, C. Pomelli, J.W. Ochterski, P.Y. Ayala, K. Morokuma, G.A. Voth, P. Salvador, J.J. Dannenberg, V.G. Zakrzewski, S. Dapprich, A.D. Daniels, M.C. Strain, O. Farkas, D.K. Malick, A.D. Rabuck, K. Raghavachari, J.B. Foresman, J.V. Ortiz, Q. Cui, A.G. Baboul, S. Clifford, J. Cioslowski, B.B. Stefanov, G. Liu, A. Liashenko, P. Piskorz, I. Komaromi, R.L. Martin, D.J. Fox, T. Keith, M.A. Al-Laham, C.Y. Peng, A. Nanayakkara, M. Challacombe, P.M.W. Gill, B. Johnson, W. Chen, M.W. Wong, C. Gonzalez, J.A. Pople, Gaussian 03, Gaussian Inc., Wallingford, CT, 2004.

[27] W.D. Cornell, P. Cieplak, C.I. Bayly, I.R. Gould, K.M. Merz, D.M. Ferguson, D.C. Spellmeyer, T. Fox, J.W. Caldwell, P.A. Kollman, A 2Nd generation force-field for the simulation of proteins, nucleic-acids, and organic-molecules, J. Am. Chem. Soc. 117 (1995) 5179–5197.

[28] W.L. Jorgensen, J. Chandrasekhar, J.D. Madura, R.W. Impey, M.L. Klein, Comparison of simple potential functions for simulating liquid water, J. Chem. Phys. 79 (1983) 926–935.

[29] J.P. Ryckaert, G. Ciccotti, H.J.C. Berendsen, Numerical-integration of Cartesian equations of motion of a system with constraints—molecular-dynamics of *n*-alkanes, J. Comput. Phys. 23 (1977) 327–341.

[30] A.H. Juffer, E.F.F. Botta, B.A.M. Vankeulen, A. Vanderploeg, H.J.C. Berendsen, The electric-potential of a macromolecule in a solvent—a fundamental approach, J. Comput. Phys. 97 (1991) 144–171.

[31] W. Humphrey, A. Dalke, K. Schulten, VMD: visual molecular dynamics, J. Mol. Graph. 14 (1996) 33–38, 27–8.

[32] J. Aqvist, J. Marelius, The linear interaction energy method for predicting ligand binding free energies, Comb. Chem. High Throughput Screen 4 (2001) 613–626.

[33] T. Hansson, J. Marelius, J. Aqvist, Ligand binding affinity prediction by linear interaction energy methods, J. Comput. Aided Mol. Des. 12 (1998) 27–35.

[34] T. Fujimura, H. Sakuma, A. Ohkubo-Suzuki, I. Aramori, S. Mutoh, Unique properties of coactivator recruitment caused by differential binding of FK614, an antidiabetic agent, to peroxisome proliferator-activated receptor gamma, Biol. Pharm. Bull. 29 (2006) 423–429.

[35] C. Bissantz, G. Folkers, D. Rognan, Protein-based virtual screening of chemical databases. 1: Evaluation of different docking/scoring combinations, J. Med. Chem. 43 (2000) 4759–4767.

[36] G.L. Warren, C.W. Andrews, A.M. Capelli, B. Clarke, J. LaLonde, M.H. Lambert, M. Lindvall, N. Nevins, S.F. Semus, S. Senger, G. Tedesco, I.D. Wall, J.M. Woolven, C.E. Peishoff, M.S. Head, A critical assessment of docking programs and scoring functions, J. Med. Chem. 49 (2006) 5912–5931.

[37] J. Wang, R. Dixon, P.A. Kollman, Ranking ligand binding affinities with avidin: a molecular dynamics-based interaction energy study, Proteins 34 (1999) 69–81.

[38] O.A. Gani, O.A. Adekoya, L. Giurato, F. Spyrakis, P. Cozzini, S. Guccione, J.O. Winberg, I. Sylte, Theoretical calculations of the catalytic triad in short-chain alcohol dehydrogenases/reductases, Biophys. J. 94 (2008) 1412–1427.

[39] D.J. Parks, N.C. Tomkinson, M.S. Villeneuve, S.G. Blanchard, T.M. Willson, Differential activity of rosiglitazone enantiomers at PPAR gamma, Bioorg. Med. Chem. Lett. 8 (1998) 3657–3658.

[40] T. Sohda, K. Mizuno, Y. Kawamatsu, Studies on antidiabetic agents. VI: Asymmetric transformation of (+/−)-5-[4-(1-methylcyclohexylmethoxy)benzyl]-2,4-thiazolidinedione(ciglitazone) with optically active 1-phenylethylamines, Chem. Pharm. Bull. (Tokyo) 32 (1984) 4460–4465.

[41] G.D. Barish, V.A. Narkar, R.M. Evans, PPAR delta: a dagger in the heart of the metabolic syndrome, J. Clin. Invest. 116 (2006) 590–597.

[42] I.G. Schulman, G. Shao, R.A. Heyman, Transactivation by retinoid X receptor-peroxisome proliferator-activated receptor gamma (PPARgamma) heterodimers: intermolecular synergy requires only the PPARgamma hormone-dependent activation function, Mol. Cell. Biol. 18 (1998) 3483–3494.

[43] A.I. Shulman, C. Larson, D.J. Mangelsdorf, R. Ranganathan, Structural determinants of allosteric ligand activation in RXR heterodimers, Cell 116 (2004) 417–429.

[44] H.E. Xu, M.H. Lambert, V.G. Montana, K.D. Plunket, L.B. Moore, J.L. Collins, J.A. Oplinger, S.A. Kliewer, R.T. Gampe Jr., D.D. McKee, J.T. Moore, T.M. Willson, Structural determinants of ligand binding selectivity between the peroxisome proliferator-activated receptors, Proc. Natl. Acad. Sci. U.S.A. 98 (2001) 13919–13924.

[45] R.T. Nolte, G.B. Wisely, S. Westin, J.E. Cobb, M.H. Lambert, R. Kurokawa, M.G. Rosenfeld, T.M. Willson, C.K. Glass, M.V. Milburn, Ligand binding and co-activator assembly of the peroxisome proliferator-activated receptor-gamma, Nature 395 (1998) 137–143.

[46] H.E. Xu, M.H. Lambert, V.G. Montana, D.J. Parks, S.G. Blanchard, P.J. Brown, D.D. Sternbach, J.M. Lehmann, G.B. Wisely, T.M. Willson, S.A. Kliewer, M.V. Milburn, Molecular recognition of fatty acids by peroxisome proliferator-activated receptors, Mol. Cell 3 (1999) 397–403.